1995ICRC....4.1013S

Observations of Geomagnetically Trapped Anomalous Cosmic Rays

R. S. Selesnick[1], R. A. Mewaldt[1], E. C. Stone[1], G. M. Mason[2],
J. E. Mazur[2], J. B. Blake[3], M. D. Looper[3], B. Klecker[4], D. Hovestadt[4]
[1] *California Institute of Technology, Pasadena, CA 91125, USA*
[2] *University of Maryland, College Park, MD 20742, USA*
[3] *The Aerospace Corporation, El Segundo, CA 90245, USA*
[4] *Max-Planck-Institut für extraterrestrische Physik, D 8046 Garching, FRG*

Abstract

Energy spectra from three instruments on SAMPEX of geomagnetically trapped anomalous cosmic ray O and Ne with ~1 to 50 MeV/nucleon are peaked near the local western geomagnetic cutoff energy, sharply decreasing above and gradually decreasing below this energy. They are in reasonable agreement with model spectra based on the trapping theory.

Measurements of geomagnetically trapped anomalous cosmic rays (ACRs) were first made by the Cosmos satellites in the 1980s [1] and during the present solar cycle by SAMPEX after its launch in 1992 [2]. Energy spectra for oxygen ions with 16 to ~50 MeV/nucleon from the MAST instrument [3] on SAMPEX were reported later [4], along with the pitch-angle and spatial distributions. These results were supplemented [5] by data from the SAMPEX HILT sensor [6] which covers a somewhat lower energy range of 8 to 29 MeV/nucleon.

In mid-1994 the SAMPEX pointing strategy was modified to increase the number of trapped particles observed, particularly at energies $\gtrsim$1 MeV/nucleon with the LICA sensor [7], which has a more directional response and smaller geometry factor. In this report we describe the energy spectra of trapped ACR O and Ne obtained by combining data from all three SAMPEX instruments, covering energies from ~1 to 50 MeV/nucleon.

The data analysis technique is similar to the one used previously [4]. The intensity is calculated at a fixed dipole radius R, defined in terms of the local magnetic field B and the L shell by

$$\frac{B}{B_0} = \frac{L^3}{R^3}\left(4 - \frac{3R}{L}\right)^{1/2} \tag{1}$$

where $B_0 = M/(La)^3$ is the dipole equatorial field, $M = 7.82 \times 10^{15}$ Tm^3 is the Earth's dipole moment and $a = 6371.2$ km its radius. A value of $R = 1.29$, near the maximum value encountered by SAMPEX during its orbit, is adopted here. (In the previous analysis of the MAST data [4] a value of $R = 1.30$ was used because B_0 was derived from the IGRF magnetic field model, rather than the dipole value used here and for the HILT analysis [5].)

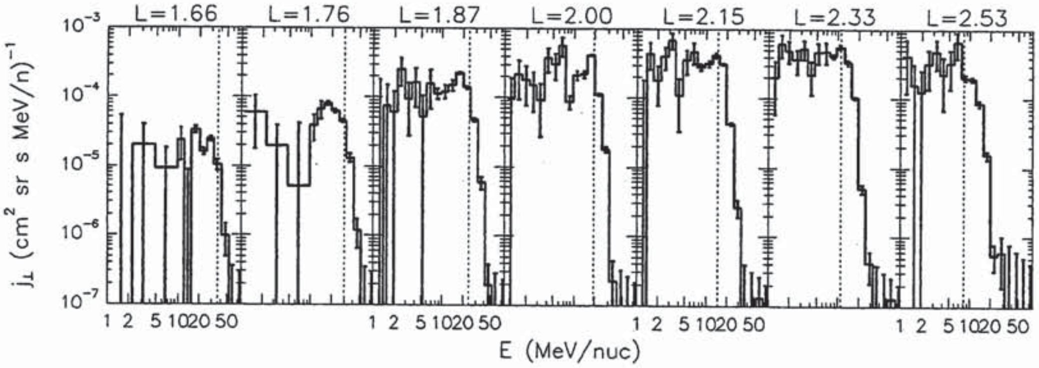

Figure 1: Energy spectra of trapped O for the indicated L shells derived from the SAMPEX data. The energies of the singly charged ion local dipole western geomagnetic cutoff are shown by dotted lines.

The intensity j at $R = 1.29$ is calculated by assuming that it is a separable function $j = U(E, L)V(\alpha)W(t)$, where E is kinetic energy per nucleon, α is pitch angle transformed to $R = 1.29$, and t is time. The three functions U, V, and W are evaluated by an iterative technique taking into account the appropriate exposure factor for each instrument, which is a function of effective area, angular response, pointing direction, magnetic field direction, and livetime. In cases where an energy bin is covered by more than one instrument, averages appropriately weighted by their respective standard errors and exposure factors are used. The functions are normalized so that the energy spectrum U represents the intensity perpendicular to the magnetic field at $R = 1.29$.

Due to operational factors the data coverage is not the same for each instrument. However, all times during the period from July 1992 to February 1995 are covered by at least one instrument, so under the assumption of separable variables the energy spectra are properly normalized and represent an average over the entire period.

The pitch-angle distribution $V(\alpha)$ of the trapped ACRs has been reported previously [4] and is not shown here. The time dependence $W(t)$ continues to show an increase in the trapped intensity as solar minimum approaches, with a factor of $\sim$3 to 4 increase in the $\sim$2.5 years since the SAMPEX launch, comparable to the observed increase in the interplanetary ACR intensity [8].

The energy spectra $U(E, L)$ from the three instruments combined are shown in Figure 1 for trapped oxygen. Each panel of Figure 1 represents the spectrum measured in a 2° invariant latitude ($\cos^{-1} L^{-1/2}$) bin. The results are consistent with those reported previously for the MAST [4] and HILT [5] instruments independently. The data from LICA provide new information on the spectra below the nominal energies of the western geomagnetic cutoff that are also shown in the figure.

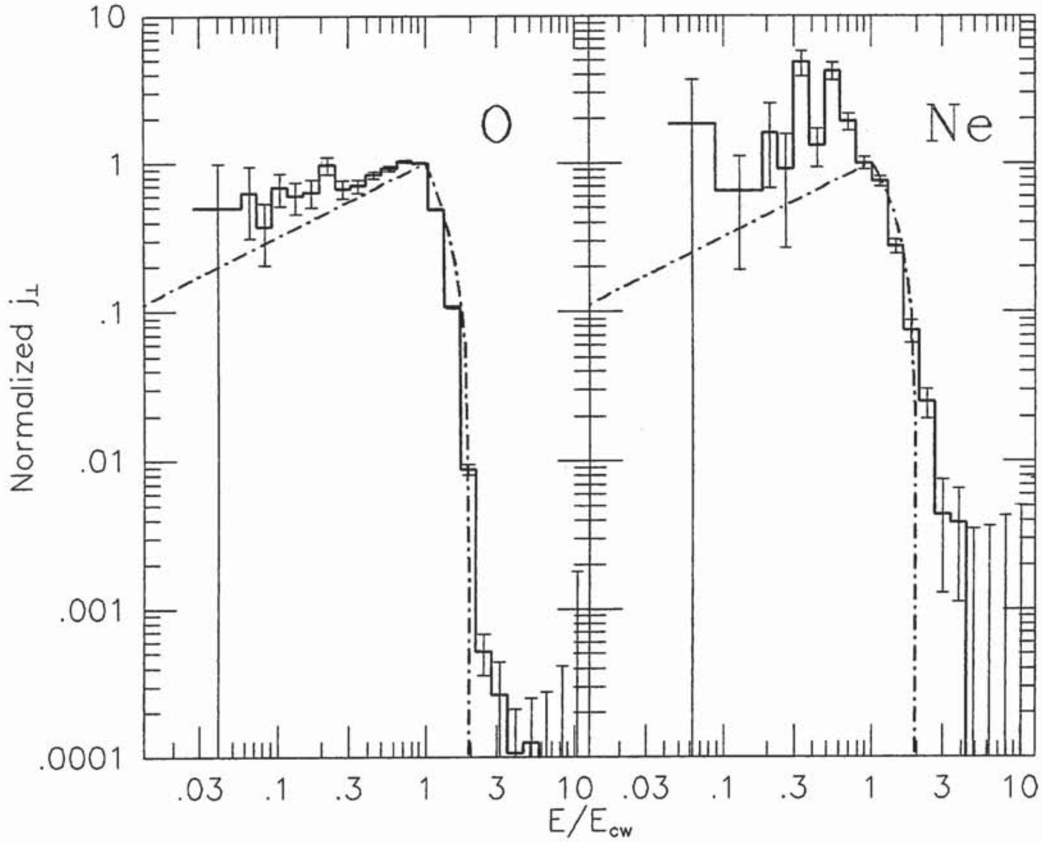

Figure 2: Spectra of trapped ACR O and Ne for the whole range of L shells shown in Figure 1. The energy is normalized by the local western geomagnetic cutoff energy. Model spectra, described in the text, are shown by the dash-dot curves.

The results in Figure 1 confirm that the geomagnetic cutoff is associated with the energy of the maximum trapped ACR intensity, as reported previously [5]. To illustrate this further we have reanalyzed the data under the assumption that the intensity is separable in four variables, E/E_{cw}, L, α, and t, after the energy is normalized to the local western geomagnetic cutoff energy of singly charged ions, E_{cw}. This has the additional advantage of improving the statistics for the energy spectrum because all of the observed particles between invariant latitudes of 38° and 52° are included in a single spectrum. The results for both O and Ne, normalized to the intensity at $E/E_{cw} = 1$, are shown in Figure 2. The absolute intensity of Ne is lower than that of O by a factor varying from ~10 at $L = 1.66$ to ~25 at $L = 2.0$.

A simple model of the trapped ACR intensity, based on particle trapping at $E > E_{cw}$ and subsequent energy loss in the residual atmosphere, and similar to other models [9,10], is [4]

$$j(E) = j_0 \frac{\tau(E_1)}{\tau_B(E)} \left(e^{-\max(E,E_{cw})/E_1} - e^{-E_{\max}/E_1} \right) \tag{2}$$

where j_0 is related to the interplanetary ACR intensity and the probability of stripping electrons from a singly charged ACR in the upper atmosphere, τ is the energy loss lifetime ($j_0\tau(E_1)$ is a normalizing factor for the energy spectrum), τ_B is the bounce period, E_1 is the e-folding energy of the ACR spectrum after trapping, and $E_{\max}$ is the maximum energy for particle trapping. Model spectra of this type, assuming $E_1 = 8$ MeV/nucleon and a value of $E_{\max}$ based on a maximum value of 0.9 for the product ϵQ of the adiabiticity parameter and initial charge state of the trapped particles [4], are shown in Figure 2 for comparison with the data. For $E > E_{cw}$ the model normalized energy spectra vary with L, and averages over the range of L appropriate to the data are shown in Figure 2.

In conclusion, the energy spectra shown if Figures 1 and 2 are clearly organized by the geomagnetic cutoff, rising with energy below the cutoff energy and sharply falling with energy above the cutoff energy. These trends are readily apparent when the energy is normalized by the local western cutoff energy. The simple model spectra shown in Figure 2 predict this behavior, confirming that the data are in reasonable agreement with expectations based on the theory for trapping interplanetary ACRs. The data show some excess intensity over the model predictions below the normalized cutoff energy which is probably is due to the simplicity of the model.

Acknowledgements. This work was supported by NASA under contract NAS5-30704 and grant NAGW-1919, by NASA Cooperative Agreement 26979B at The Aerospace Corporation, and by the Bundesministerium für Forschung und Technologie, Germany under grant 50 OC90021.

References

[1] Grigorov, N.L, et al., Geophys. Res. Lett., **18** (1991) 1959.
[2] Cummings, J.R., et al., Geophys. Res. Lett., **20** (1993) 2003.
[3] Cook, W.R., at al., IEEE Trans. Geosc. Remote Sens., **31** (1993) 557.
[4] Selesnick, R.S., et al., J. Geophys. Res., in press (1995).
[5] Looper, M.D., et al., submitted to J. Geophys. Res. (1995).
[6] Klecker, B., et al., IEEE Trans. Geosc. Remote Sens., **31** (1993) 542.
[7] Mason, G.M., et al., IEEE Trans. Geosc. Remote Sens., **31** (1993) 549.
[8] Mewaldt, R.A., et al., this conference.
[9] Blake, J.B., 21st ICRC, **7** (1990) 30.
[10] Tylka, A.J., 23rd ICRC, **3** (1993) 436.